13th World Conference on Earthquake Engineering
Vancouver, B.C., Canada
August 1-6, 2004
Paper No. 574

THE USE OF POWER FOR THE CHARACTERIZATION OF EARTHQUAKE GROUND MOTIONS

Kenneth ELWOOD[1] and Erik NIIT[2]

SUMMARY

Power, defined as the time rate of change of energy, has received little or no attention in the literature as a useful parameter for selecting critical ground motions for seismic design. Power can be used to distinguish between distant and near-fault ground motions which may have approximately the same maximum input energy. Furthermore, the rate at which energy is dissipated through either damping or yielding of the structure can be determined by calculating the damping and hysteretic power terms. This study investigates the characteristics of power time histories for selected ground motions and an elastic-perfectly-plastic SDOF oscillator. Power spectra are also developed to investigate the variation of the maximum input power with the period of the structure and the assumed hysteretic model. It is noted that short period structures tend to experience a constant input power regardless of the ductility demand.

INTRODUCTION

The use of energy concepts in earthquake-resistant design was first proposed by Housner [1]; however, little research has done in this area until the past 20 years. Uang and Bertero [2] proposed the use of energy spectra, developed from single degree of freedom (SDOF) systems, for earthquake-resistant design and proposed methods of evaluating the energy capacity of structural materials. To date, the majority of research has been directed toward correlating the input energy to the severity of the earthquake ground motion and the development of damage indices based, in part, on hysteretic energy demand. Thus far, no significant research has been undertaken to study the rate of energy input into the structure (i.e. input power) and the rate at which energy is balanced by the various storage and dissipation mechanisms in the structure (i.e. hysteretic, damping, kinetic, and strain power). Since pulse-type and long-duration ground motions can impart the same total input energy to a system, while requiring the energy to be dissipated at different rates, it may be beneficial to quantify and characterize the earthquake power when selecting critical ground motions. Although not considered explicitly in calculations, the concept of power has been discussed by Housner and Jennings [3]: “If energy is fed to a structure at a sufficiently slow rate [i.e. low power], the dissipation due to damping will prevent the structural members from becoming overstressed, but during a high rate of energy input [i.e. high power] the dissipation by damping may be

[1] Assistant Professor, Department of Civil Engineering, University of British Columbia, Vancouver, Canada
[2] Graduate Student, Department of Civil Engineering, University of British Columbia, Vancouver, Canada

inadequate to hold the energy level in the structure below the threshold of damage, and then plastic deformation, cracking, etc. may result."

The objective of this paper is thus to characterize near-fault (or pulse-type) ground motions and long-duration ground motions, using the concept of earthquake power, and to a lesser extent, earthquake energy. This will be accomplished through a description of the characteristics of power time histories and power spectra. Earthquake power will be introduced for an elastic-perfectly-plastic (EPP) SDOF oscillator subjected to a series of recorded pulse-type and long-duration ground motions. The influence of the assumed hysteretic model will also be investigated.

This paper will present the use of power demand as a measure of the severity and damage potential of earthquakes. In this context, power is viewed as the rate of change of energy and should not be confused with the power spectral density, which relates to the frequency content of an earthquake ground motion.

ENERGY AND POWER EQUATIONS

Energy

The relative energy balance equation for a SDOF oscillator is determined by integrating the equation of motion with respect to relative displacement, *u*, Uang and Bertero [2].

$$\int_u m\ddot{u}du + \int_u c\dot{u}du + \int_u f_S du = -\int_u m\ddot{u}_g du \tag{2.1}$$

For Eq. (2.1), m is the mass, c is the coefficient of viscous damping, f_S is the restoring force, $\ddot{u}_g$ is the ground acceleration, and u, $\dot{u}$, and $\ddot{u}$ are the relative displacement, velocity, and, acceleration of the mass, respectively. It should be noted that the restoring force, f_S represents the spring force of the inelastic system. From the left to the right side of Eq. (2.1), the first term is referred to as the relative kinetic energy E_K, the second term is the damping energy, E_D, and the third term represents the absorbed energy and consists of the elastic strain energy, E_S, and the inelastic hysteretic energy, E_H. The term on the right-hand side of Eq. (2.1) corresponds to the relative input energy of the ground motion, E_I, or the work done by the effective earthquake force, $-m\ddot{u}_g$. Hence, the energy balance equation can expressed as follows,

$$E_K + E_D + E_S + E_H = E_I \tag{2.2}$$

For a non-stiffness degrading system, the strain energy can be expressed as:

$$E_S = \frac{(f_S)^2}{2k} \tag{2.3}$$

where k is the initial elastic stiffness of the system. For an EPP hysteretic model, the hysteretic energy can be expressed concisely as the product of the yield force level, F_Y, and the total cumulative plastic displacements, Δ_p^{cum},

$$E_H = F_Y \cdot \Delta_p^{cum} \tag{2.4}$$

The differences between the absolute and relative formulations of the energy balance equation are discussed in detail by Uang and Bertero [2]. This study will concentrate on the relative formulation for two reasons. First, relative energy terms may be considered more useful since the spring and damping forces in a structure are related to the relative displacements and velocities. Second, for long period structures the absolute input energy will approach zero, and hence, is not useful for the design of such structures. For very short period structures the relative input energy will approach zero; however, these structures require a strength-based design to avoid excessive ductility demands, and hence, energy concepts may be inappropriate. Thus, for the remainder of this paper any reference to input energy and kinetic energy will refer to the relative input and kinetic energies.

Power

Power is physically defined as the time rate of change of energy. The relative power equation governing the motion of the SDOF oscillator may be formulated by differentiating Eq. (2.1) with respect to time:

$$\frac{d}{dt}\int_u m\ddot{u}du + \frac{d}{dt}\int_u c\dot{u}du + \frac{d}{dt}\int_u f_S du = -\frac{d}{dt}\int_u m\ddot{u}_g du \tag{2.5}$$

Carrying out the integration above,

$$m\ddot{u}\dot{u} + c\dot{u}^2 + f_S\dot{u} = -m\ddot{u}_g\dot{u} \tag{2.6}$$

Similar to the energy terms expressed in Eq. (2.2), the terms on the left-hand side of the equation correspond to the relative kinetic power, P_K, the damping power, P_D, and the absorbed power which consists of the elastic strain power, P_S, and the inelastic hysteretic power, P_H. The term on the right-hand side of the equation defines the relative input power of the ground motion, P_I. As with the energy balance, the power balance can be rewritten as:

$$P_K + P_D + P_S + P_H = P_I \tag{2.7}$$

Note that the strain and hysteretic power terms for an EPP system can be calculated directly by differentiation of Eq. (2.3) and Eq. (2.4), respectively,

$$P_S = \frac{d}{dt}\left[\frac{(f_S)^2}{2k}\right] = \frac{f_S}{k}\frac{d}{dt}(f_S) \tag{2.8}$$

$$P_H = \frac{d}{dt}E_H = \frac{d}{dt}(F_Y \cdot \Delta_{cum}) = F_Y\frac{d}{dt}(\Delta_{cum}) \tag{2.9}$$

The spectral analysis program Bispec [4] was used throughout this study to calculate the numerical results.

SELECTION OF GROUND MOTIONS

For this study, two broad classes of ground motions have been considered: near-fault records from crustal earthquakes to represent *pulse-type* ground motions (Table 1), and records from subduction-type earthquakes to represent *long-duration* ground motions (Table 2). All ground motions were selected from records used for the SAC Steel Project [5] and have a return period of approximately 475 years.

Table 1. Pulse-type ground motions [5].

SAC Name	Earthquake	Station	Magnitude	Scale	Distance (km)	Duration[1] (s)	Year
NF01	Tabas		7.4	1.00	1.92	43.18	1978
NF03	Loma Prieta	Los Gatos	7.0	1.00	5.6	16.42	1989
NF05	Loma Prieta	Lex. Dam	7.0	1.00	10.08	7.10	1989
NF07	C. Mendocino	Petrolia	7.1	1.00	13.6	20.96	1992
NF09	Erzincan		6.7	1.00	3.2	12.26	1992
NF11	Landers		7.3	1.00	1.76	34.29	1992
NF13	Northridge	Rinaldi	6.7	1.00	12	14.87	1994
NF15	Northridge	Olive View	6.7	1.00	10.24	11.34	1994
NF17	Kobe	Kobe	6.9	1.00	5.44	17.62	1995
NF19	Kobe	Takatori	6.9	1.00	6.88	23.10	1995

1. "Duration" calculated based on bracketed duration for 0.05g [6].

Table 2. Long-duration ground motions [5].

SAC Name	Earthquake	Station	Magnitude	Scale	Distance (km)	Duration[1] (s)	Year
SE05	West Washington	Olympia	6.5	1.86	89.6	46.64	1949
SE06	West Washington	Olympia	6.5	1.86	89.6	31.38	1949
SE07	West Washington	Seattle Army Base	6.5	5.34	128	63.13	1949
SE08	West Washington	Seattle Army Base	6.5	5.34	128	64.91	1949
SE15	East Washington	Tacoma County	7.1	8.68	96	44.00	1965
SE16	East Washington	Tacoma County	7.1	8.68	96	47.72	1965
SE17	Chile	Llolleo	8.0	1.24	67.2	78.75	1985
SE18	Chile	Llolleo	8.0	1.24	67.2	78.58	1985
SE19	Chile	Vina del Mar	8.0	1.69	67.2	73.13	1985
SE20	Chile	Vina del Mar	8.0	1.69	67.2	71.78	1985

1. "Duration" calculated based on bracketed duration for 0.05g [6].

ENERGY AND POWER TIME HISTORIES

Energy and power time histories were produced for an SDOF oscillator with a period of 0.8 seconds and 5% viscous damping. The non-linear characteristics of the system were modeled using an EPP hysteretic model with a yield force level defined by a normalized strength of unity. (The normalized strength is given by $\eta = F_Y/(m \cdot PGA)$, where PGA refers to the peak ground acceleration).

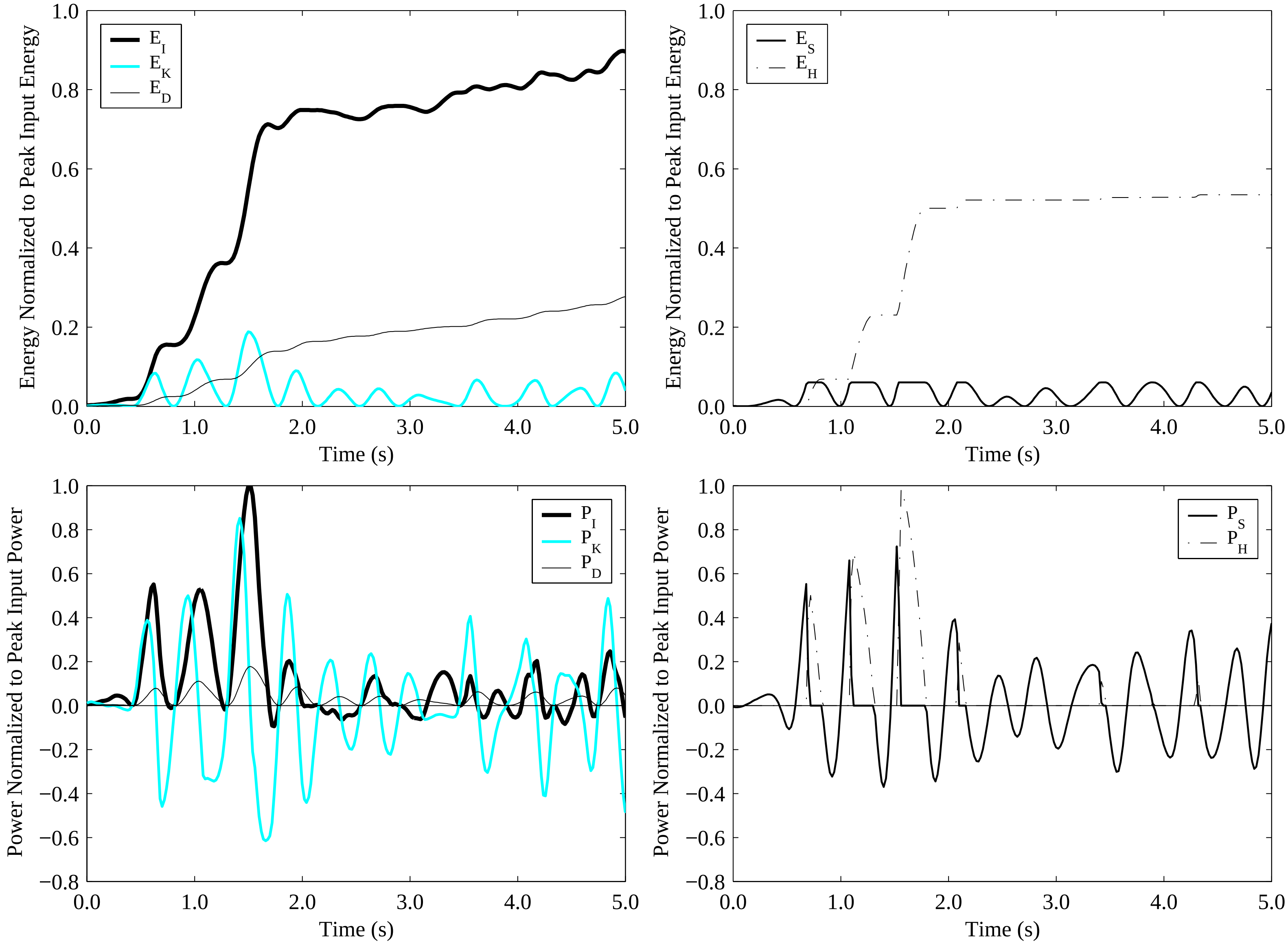

Figure 1. Non-linear energy and power time history for NF17 ground motion (Kobe, 1995) (T = 0.8 sec, ζ = 5%).

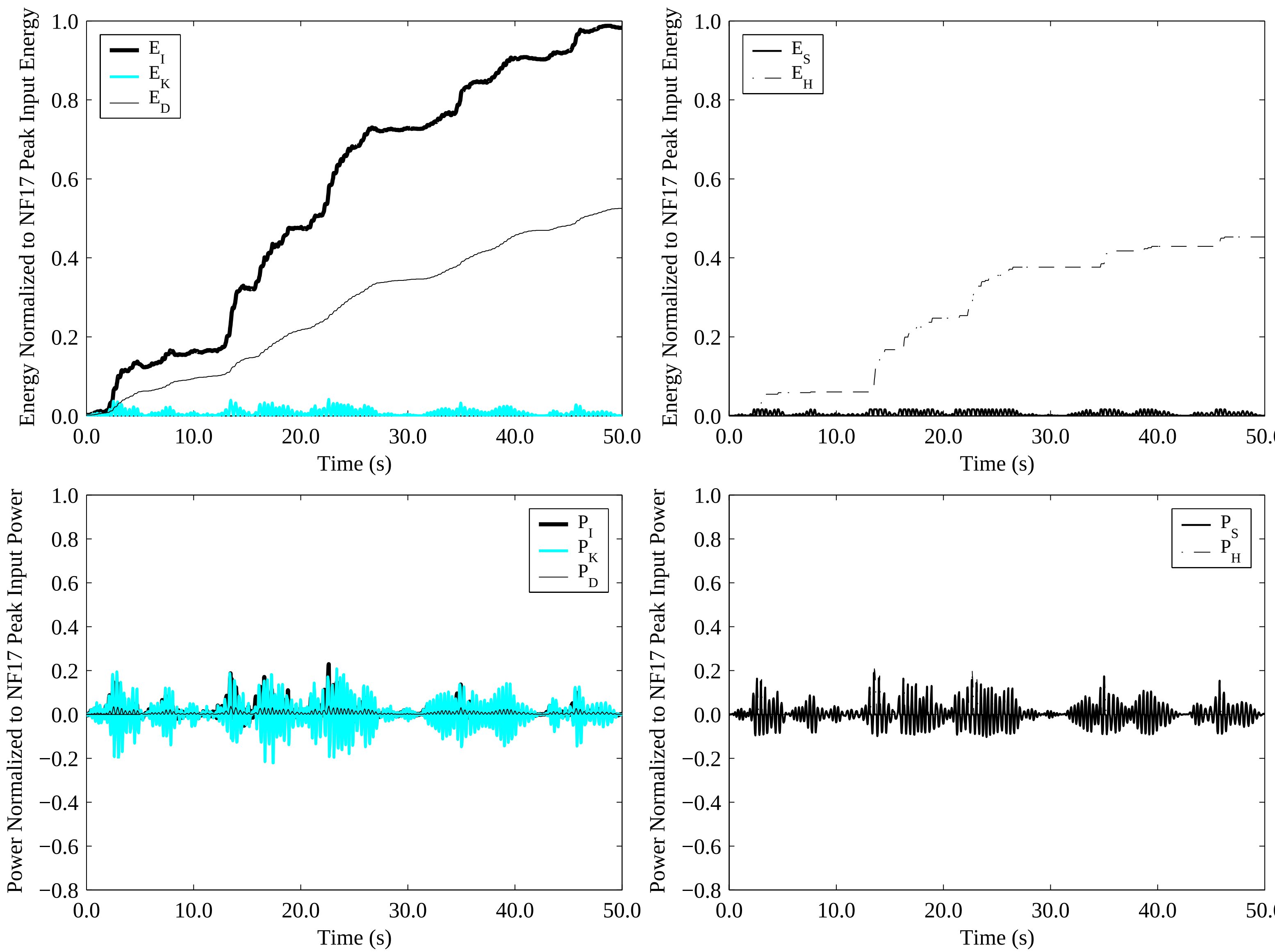

Figure 2. Non-linear energy and power time history for SE19 ground motion (Vina del Mar, 1985) (T = 0.8 sec, ζ = 5%).
(Peak input energy equal to input energy for NF17 ground motion. Power terms normalized to peak input power for NF17 ground motion)

It should be noted that the observations presented may depend on the chosen characteristics of the particular systems, in particular the period of the SDOF, the hysteretic model, and ground motions evaluated. The influence of such characteristics will be discussed in subsequent sections on energy and power spectra.

The energy and power time histories for the NF17 pulse-type ground motion and the SE19 long-duration ground motion are presented in Figures 1 and 2. The acceleration amplitude of the SE19 ground motion was scaled by 1.05 to achieve the peak input energy of the NF17 ground motion. To facilitate comparison of the results, the energy and power time histories for both ground motions were normalized to the peak input energy and the peak input power for the NF17 ground motion. It should be noted that the response of both systems was computed with a normalized strength of 1.0; however the PGA of the NF17 ground motion was nearly twice that of the SE19 ground motion, and, for the same mass, the NF17 yield strength was thus nearly twice that of the SE19 yield strength.

The NF17 and SE19 energy time histories illustrate some of the characteristic differences between pulse and long duration ground motions. For example, the SE19 response requires approximately forty-five seconds, nine times longer than the NF17 response, to input the same amount of energy into the system. The proportion of the input energy dissipated by hysteretic energy is much larger for the NF17 response than for the SE19 response (in which the damping and hysteretic energy increase at roughly the same rate). The hysteretic energy developed in the SE19 ground motion is built up over a much larger number of yielding events than in the NF17 response.

Intuitively, the NF17 ground motion must impart the same amount of input energy as the SE19 ground motion over a much shorter time thus requiring a faster rate of energy delivery (i.e. higher power). The NF17 and SE19 power time histories indicate that the peak value of the SE19 input power is much smaller than the peak value of the NF17 input power. Indeed, all of the power terms in the SE19 power time history are approximately 25% of their value in the NF17 power time history. It should be noted, however, that the P_H/P_I ratio is only slightly higher, while the P_K/P_I and P_S/P_I are actually slightly lower for the NF17 response terms when compared with the SE19 response. This suggests that each power term maintains an approximate proportion of the input power regardless of the ground motion, an observation that will be discussed further below.

The power time history for the NF17 ground motion, shown in Figure 1, can be used to illustrate several interesting characteristics of the individual power terms. From the lower right plot of Figure 1 it is clear that only one of the hysteretic and strain power terms is active at any one time; at the moment of yielding, the strain power drops to zero while the hysteretic power spikes to the same power magnitude as the strain power term immediately prior to yielding. The variation in time of the strain and hysteretic power terms can be readily understood by considering the sum of the strain and hysteretic power terms, referred to herein as the "spring power". The kinetic power term and the spring power term are out of phase by approximately 180˚. The damping power, which is relatively small, is out of phase with the kinetic and spring terms by approximately 90˚. A negative increase in the strain power term corresponds to unloading of the SDOF elastically.

It is also interesting to note from Figure 1 that all of the power terms converge to zero at the same time. This observation can be explained by noting that each power term in Eq. (2.6) is a function of the velocity. Thus, if the velocity approaches zero, all of the power terms must also approach zero. The damping power will always maintain a positive value due to the dependence on the square of the velocity. While the spring power is directly related to the velocity and must change signs when the velocity changes signs, the hysteretic power, according to Eq. (2.9), will always be positive since the time derivative of the cumulative plastic displacements is also always positive. The hysteretic power will be zero when the SDOF unloads elastically at a peak in the displacement, and hence, at zero velocity. Thus, the spring power and hysteretic power will both be zero when the velocity is zero, thereby requiring the strain power to also be zero. Also observed from Eq. (2.6), the input power is directly related to the ground acceleration and must necessarily become zero when the ground motion ceases.

The acceleration records of five ground motions were scaled such that the peak input energy matched that of the NF17 response for three normalized strength values (with T = 0.8sec). The relationship between the peak input power for each ground motion, at a given normalized strength, and the peak input power of the NF17 response is shown in Table 3. The results suggest some dependence of input power on the ground motion. The input power of the long duration ground motions (SE07, SE17, and SE19) is consistently less than the input power of the pulse-type ground motions (NF13, NF17, and NF19) regardless of the normalized strength. This observation suggests that high values of input power may characterize pulse-type ground motions, while low values of input power may characterize long-duration ground motions.

The results in Table 3 further suggest that the normalized strength influences the magnitude of P_S/P_I, P_H/P_I, and P_K/P_I. The proportion P_D/P_I, however, appears to be roughly independent of the normalized strength and the characteristics of the ground motion. Further analyses indicate that, regardless of period, P_D/P_I is approximately constant for ductility demands greater than 4.0. It is also worthy to note that, with the exception of P_K/P_I for SE17, the peak kinetic, strain, hysteretic, and damping power values (expressed as a fraction of the peak input power) appear to be relatively independent of the selected ground motion.

Table 3. Peak power terms for six ground motions at a constant system period of 0.8s and a specified normalized strength.

Normalized Strength	Ground Motion	Scale Factor	$P_I/P_{I,NF17}$	P_K/P_I	P_S/P_I	P_H/P_I	P_D/P_I
0.2	NF13	1.45	1.63	0.71	0.13	0.24	0.15
	NF17	1.00	1.00	0.69	0.11	0.26	0.17
	NF19	0.89	0.54	0.60	0.09	0.28	0.25
	SE07	1.69	0.16	0.75	0.14	0.28	0.15
	SE17	1.38	0.25	1.24	0.27	0.43	0.14
	SE19	1.03	0.19	0.84	0.12	0.29	0.15
0.6	NF13	1.57	1.72	0.63	0.51	0.62	0.15
	NF17	1.00	1.00	0.77	0.47	0.64	0.16
	NF19	1.19	0.45	0.58	0.62	0.74	0.13
	SE07	1.72	0.16	0.79	0.54	0.73	0.16
	SE17	1.46	0.34	1.59	0.66	0.75	0.17
	SE19	1.03	0.21	0.83	0.45	0.64	0.14
1	NF13	1.63	1.49	0.91	1.01	1.06	0.18
	NF17	1.00	1.00	0.85	0.71	0.98	0.18
	NF19	1.55	0.84	0.58	0.87	0.99	0.12
	SE07	1.85	0.19	0.98	0.99	1.15	0.19
	SE17	1.52	0.40	1.75	1.12	1.08	0.21
	SE19	1.06	0.23	0.98	0.81	0.93	0.17

ENERGY AND POWER RESPONSE SPECTRA

The previous sections investigated the power and energy response of an arbitrarily selected elastic-perfectly-plastic SDOF oscillator with a period of 0.8 seconds. Power and energy response spectra are discussed in the following sections to investigate the dependence of the maximum response on the oscillator period. The discussion presented herein is limited to the input terms; investigation of hysteretic power and energy spectra can be found elsewhere [7].

Input energy and input power spectra

It is convenient to express the input energy and input power as a dimensionless quantity. To achieve this, both terms are normalized by the input energy and input power for long period structures since both long period terms converge to a specific value depending only on the properties of the ground motion and the system mass. Recalling that the relative displacement approaches the ground displacement for long period structures, the long period input energy can be formulated as follows:

$$E_I(T \to \infty) = -\int_u m\ddot{u}_g du = \int_{u_g} m\ddot{u}_g du_g = \frac{1}{2} m\dot{u}_g^{\,2}(t) \tag{5.1}$$

Thus, the maximum long period input energy is given by,

$$E_{I,\max}(T \to \infty) = \frac{1}{2} mPGV^2 \tag{5.2}$$

where *PGV* is the peak ground velocity. Similarly, the long period input power can be formulated, from Eq. (2.6), as

$$P_I(T \to \infty) = -m\ddot{u}_g \dot{u} = m(\ddot{u}_g \dot{u}_g) \tag{5.3}$$

Finally, the maximum long period input power is given by,

$$P_{I,\max}(T \to \infty) = m(\ddot{u}_g \dot{u}_g)_{\max} \tag{5.4}$$

Note that Eq. (5.4) represents the maximum value of the product of the ground acceleration and ground velocity, not the product of peak ground acceleration, PGA, and the PGV. Since the long period input energy and input power are dependent only on the characteristics of the ground motion, their independence of system strength, hysteretic model, and other system specific parameters recommends their use as a means of quantifying the properties of ground motions. Table 4 presents the long period input energy and input power for the ground motions listed in Tables 1 and 2. Note that the long period input energy and long period input power are much larger for the pulse-type ground motions than for the long-duration ground motions, likely as a result of the larger ground acceleration and velocity amplitude characteristic of near fault ground motion.

Table 4. Long period input energy and input power for near fault and subduction event ground motions.

	E_I (kN m)	P_I (kN m/s)		E_I (kN m)	P_I (kN m/s)
NF01	107.7	991.8	SE05	8.0	122.4
NF03	261.9	1123.7	SE06	11.0	119.5
NF05	279.6	1268.9	SE07	11.6	103.5
NF07	138.6	913.6	SE08	14.9	131.5
NF09	124.5	562.1	SE15	5.9	90.7
NF11	162.2	1571.2	SE16	24.7	251.3
NF13	267.7	1783.8	SE17	19.9	245.0
NF15	130.9	903.5	SE18	12.5	245.1
NF17	226.3	1609.2	SE19	33.2	306.4
NF19	264.6	1261.6	SE20	9.6	96.7

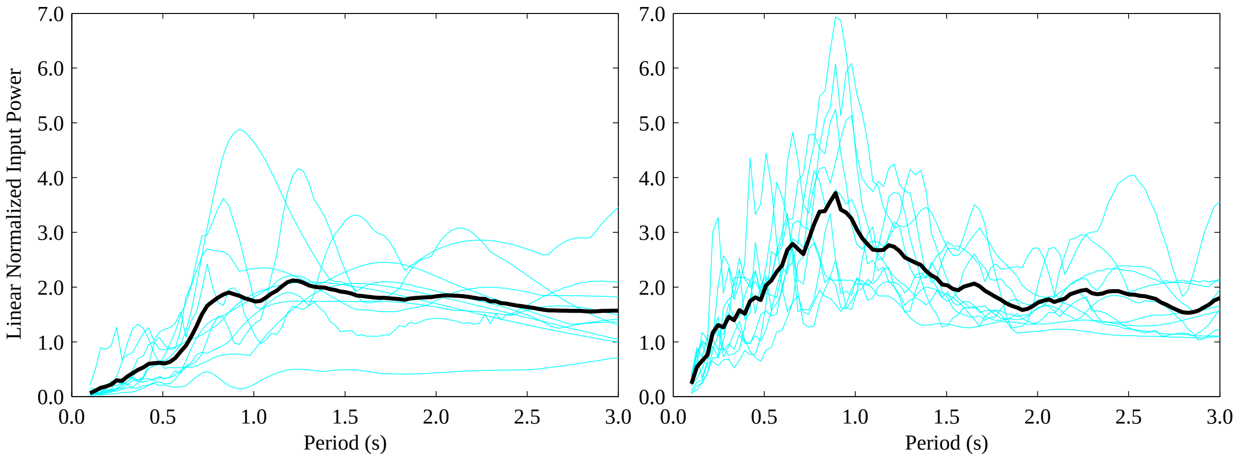

Figure 3: Averaged linear input power and individual ground motion input power for (a) pulse-type ground motions and (b) long-duration ground motions

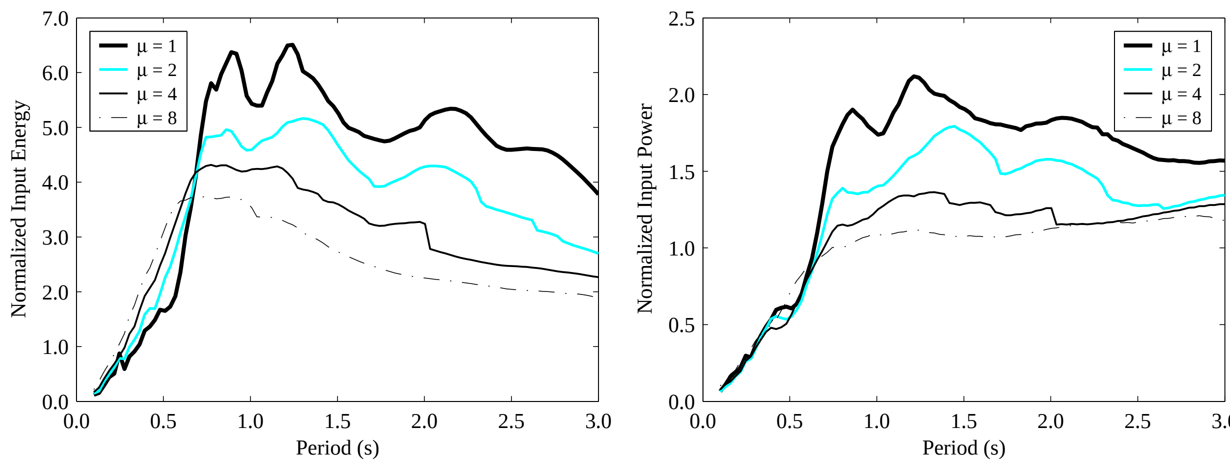

Figure 4. Constant ductility input energy and power spectra for pulse-type ground motions.

Input energy and input power spectra, normalized to the input energy and input power at long periods, were generated for the twenty ground motions presented in Table 1 and Table 2, above. The normalized near fault input energy and input power spectra were subsequently averaged together to produce a data set characteristic of pulse-type ground motions in general, and likewise for the long-duration ground motions. Figure 3 illustrates the variability between the individual linear input power spectra and the average spectra for both pulse-type and long-duration ground motions.

The averaged input energy and input power spectra for the pulse-type ground motions are presented in Figure 4. Both the non-linear input energy and input power appear to converge to the linear input energy and input power at short periods; however, this convergence is much more pronounced for the input power and occurs, according to Figure 4, for all periods less than 0.66s. From the individual ground motion spectra (not shown), the input power convergence is more pronounced for some ground motions than for others and the period at which divergence occurs varies from approximately 0.3 sec to 0.8 sec. A similar convergence was observed for the linear and non-linear averaged spectral velocity, normalized to PGV, over approximately the same period range. Recalling Eq. (2.6), it is noted that the input power and system velocity are directly related.

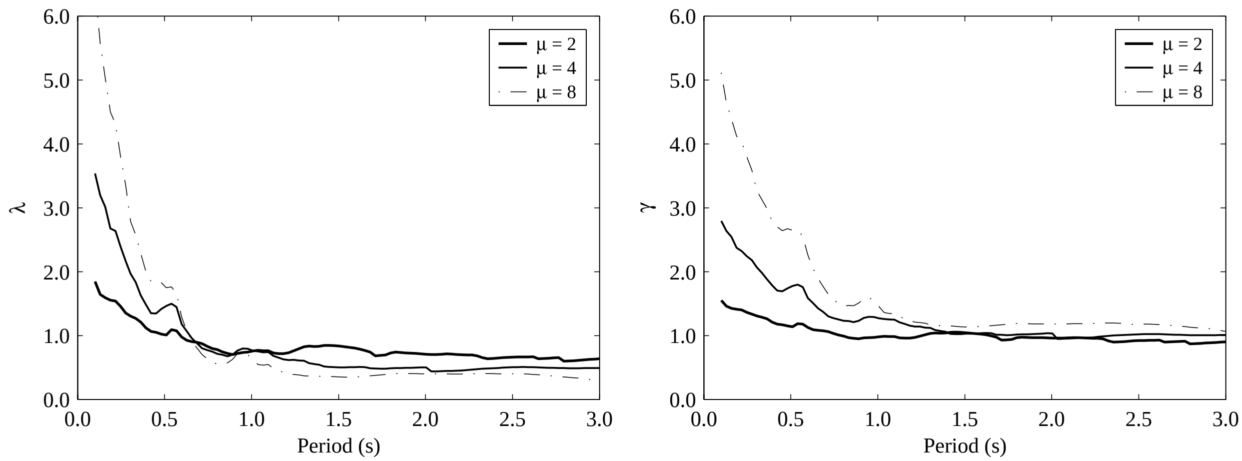

Figure 5. Monotonic hysteretic energy (λ) and normalized displacement (γ) for pulse-type ground motions

Figure 5 illustrates the applicability of equal energy and equal displacement rules [7] for the selected pulse-type ground motions. Shown on the left is the normalized monotonic energy for an EPP system, λ:

$$\lambda = \frac{F_Y u_{\max}^{inelastic} - F_Y^{\ 2} / 2k}{f_e^{\ 2} / 2k} \tag{5.5}$$

where f_e is the maximum force level of the equivalent linear system and $u_{\max}^{inelastic}$ is the peak inelastic displacement. The equal energy rule is satisfied when λ ≈ 1.0. Shown on the right of Figure 5 is the normalized displacement, γ, defined as the quotient of the peak inelastic displacement, $u_{\max}^{inelastic}$, and the peak elastic displacement of the equivalent linear system, $u_{\max}^{elastic}$:

$$\gamma = \frac{u_{\max}^{inelastic}}{u_{\max}^{elastic}} \tag{5.6}$$

The normalized displacement, γ, will approach unity when the equal displacement rule is applicable.

Comparing Figures 4 and 5, the non-linear and the linear input power are convergent during the same period range (0.1 sec to 0.66 sec) over which λ diverges dramatically. Note that λ converges to 1.0 (i.e. “equal energy”) at a period of approximately 0.66 sec, and that the linear and non-linear input power terms diverge for periods greater than 0.66 sec. Furthermore, the figures suggest that the equal energy rule has only a small range of applicability for pulse-type ground motions and that linear input power, or linear spectral velocity, may be a better means of characterizing the non-linear response of near fault ground motions at shorter periods. Note also that γ approaches unity beyond a period of 1.0 sec, supporting the equal displacement rule for long period structures.

In contrast, the averaged input power for long-duration ground motions, Figure 6, displays convergence to the linear input power up to a period of only 0.22 sec. Figure 7, showing λ and γ for the long-duration ground motions, suggests a convergence to λ = 1.0 at a period of 0.22 sec. Note also that λ remains closer to unity for a broader period range (0.22 sec to 0.6 sec) than for the pulse-type ground motions. This suggests that the equal energy principle may be satisfied for long-duration ground motions over a larger period range than for pulse-type ground motions. Figure 7 further suggests that the equal displacement rule (γ ≈ 1.0) holds for periods greater than approximately 0.6 sec.

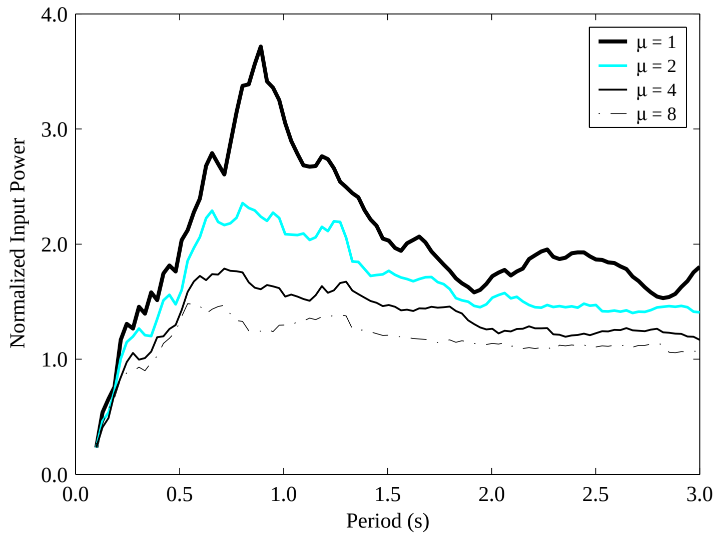

Figure 6. Averaged, normalized constant ductility input power spectra for long-duration ground motions.

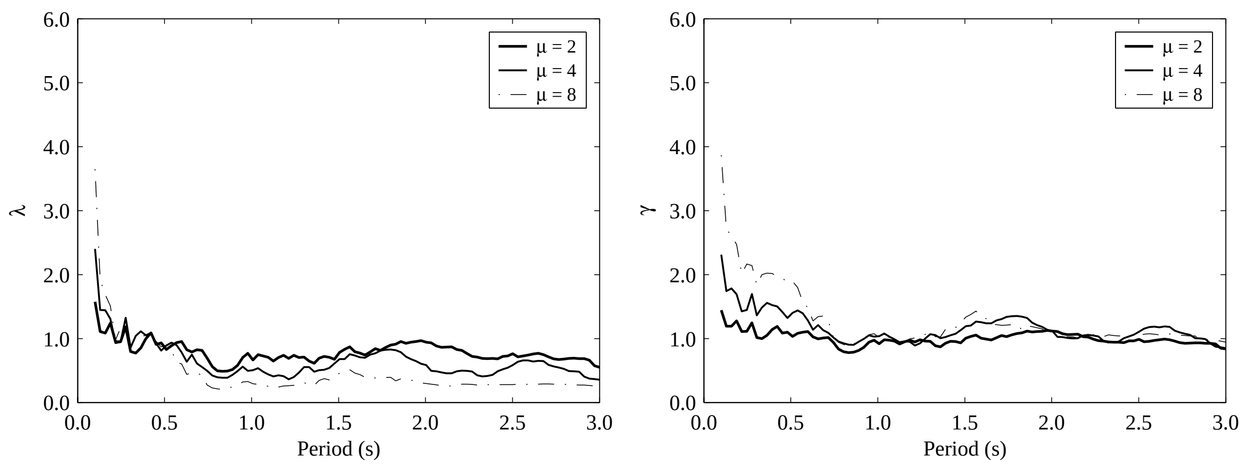

Figure 7. Monotonic hysteretic energy (λ) and normalized displacement (γ) for long-duration ground motions

In summary, for the limited ground motions considered in this study, the nonlinear SDOF response can be approximated by different linear response parameters depending on the period range and the general type of ground motion as shown in Table 5. Further study of these characteristics is required to determine if similar trends are observed for a larger database of ground motions.

Table 5. Summary of period ranges for different approximations to nonlinear response based on linear response.

Type of Ground Motion	Equal Max Input Power	Equal Max Energy	Equal Max Displacement
Pulse-type	T < 0.66 sec	0.66 sec ≤ T < 1.0 sec	T ≥ 1.0 sec
Long-duration	T < 0.22 sec	0.22 sec ≤ T < 0.6 sec	T ≥ 0.6 sec

Sensitivity to Hysteretic Model

To investigate the sensitivity of the power quantities to the assumed hysteretic model, analyses were conducted with a bilinear model with 10% strain hardening and a Clough-type stiffness degrading model [8]. Figure 8 suggests that the input power is relatively insensitive to the hysteretic model, since the input power spectra for each model is nearly identical, both in terms of salient characteristics and magnitude. The Clough hysteretic model appears to have the effect of "smoothing out" the input power spectra, but overall, the spectra correlate very well. Note that the input power spectra still converge for periods less than 0.66 sec, regardless of the assumed hysteretic model. Similarity between the results for the three hysteretic models suggests that the conclusions from the previous sections still hold for the bilinear and Clough hysteretic models.

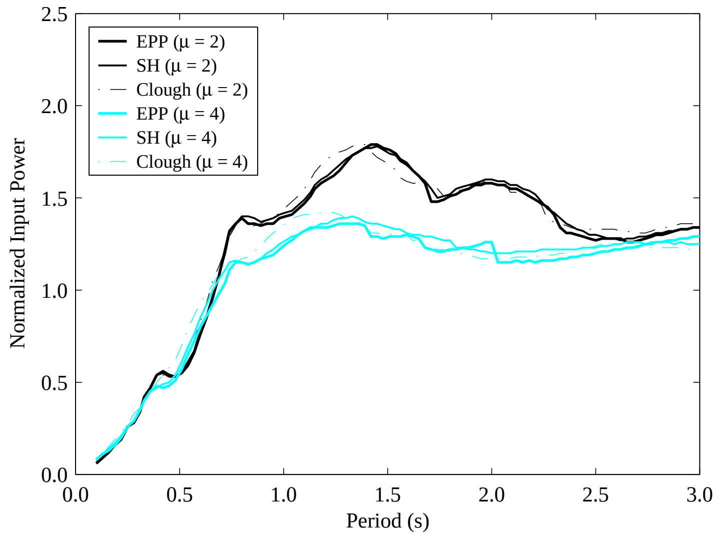

Figure 8. Input power spectra for three hysteretic models

(EPP = Elastic perfectly plastic; SH = 10% Strain hardening; Clough = Clough-type stiffness degrading)

CONCLUSIONS

This study highlights the importance of evaluating earthquake power demands in conjunction with earthquake energy demands. Generally, the input power demand was observed to depend on the nature of the ground motion, and in particular, pulse-type ground motions appear to be characterized by higher input power demand than long-duration ground motions for a constant input energy. The peak value of the strain, hysteretic, kinetic, and damping power terms normalized by the peak input power appear to be relatively independent of the characteristics of a given ground motion. However, since the input power is dependent on the ground motion, the absolute value of the power terms is also on the ground motion. The long period peak input energy and input power depend only on the ground velocity and ground acceleration and thus provide another means of characterization. It was observed that the long period input energy and input power for pulse-type ground motions tend to be considerably larger than for long-duration ground motions.

The inelastic input power was observed to converge to the linear input power for short period structures. The period range over which the non-linear and linear input power terms converge was observed to be larger for the pulse-type ground motions, compared with the long-duration ground motions. Additionally, it was noted that neither the equal energy nor equal displacement principle were valid within the period range of convergence for the input power. Further study is required to confirm if the above observations are supported by a larger sample of ground motions.

REFERENCES

1. Housner, G.W., 1956, "Limit Design of Structures to Resist Earthquakes," *Proceedings. of the 1956 World Conference on Earthquake Engineering*. Earthquake Engineering Research Institute: Oakland, California.
2. Uang, C.-M. and Bertero, V.V., 1988, "Use of Energy as a Design Criterion in Earthquake Resistant Design," *UCB/EERC-88/18*. University of California: Berkeley, California.
3. Housner, G.W. and Jennings, P.C., 1977, "The capacity of extreme ground motions to damage structures," *Structural and Geotechnical Mechanics* (ed. W.J. Hall), Prentice Hall, Englewood Cliffs, NJ, p. 102-116.
4. Hachem, M., 1999, "Bispec: Interactive Computer Program for Computation of Bidirectional Nonlinear Spectra," NISEE Software Library: Berkeley, Calif., (http://nisee.berkeley.edu/software).
5. Somerville, P.G., 1997, "Develop Suites of Time Histories – Draft Report," SAC Joint Venture Steel Project.
6. Bolt, B.A., 1969, "Duration of strong ground motion," *Proceedings. of the Fourth World Conference on Earthquake Engineering*. Santiago, Chile, pp. 1304-1315.
7. Elwood, K.J., and Niit, E.J., 2004, "The Use of Power and Energy in The Characterization of Earthquake Ground Motions," Journal of Earthquake Engineering (submitted for review).
8. Newmark, N.M. and Hall, W.J., 1982, "Earthquake Spectra and Design," *Monograph*, Earthquake Engineering Research Institute.
9. Clough, R.W., 1966, "Effect of stiffness degradation on earthquake ductility requirements", *Report 66-16*, Structural and Materials Research, Structural Engineering Laboratory, University of California, Berkeley.